J. Eng. Technol. Sci., Vol. 47, No. 6, 2015, 623-632

On the Characteristics of the Dynamic Waveform and the Change of Stress Wave Propagation Velocity in Soil Anchors

Sheng Zeng[1], Jing Zhang[1], Bing Sun[2*] & Aiyang Ma[1]

[1]School of Nuclear Resources Engineering, University of South China
(NO28, West Changsheng Road), Hengyang 421001, China
[2]Institute of Urban Construction, University of South China, Hengyang 421001, China
E-mail:sunbingzs@126.com

Abstract. This research used nondestructive testing technology to evaluate the anchorage quality of soil anchors. We first created a soil model in the laboratory and then performed a nondestructive experiment on the soil anchor using the stress wave reflection method. Our study displays variable characteristics of the acceleration response curve of a soil anchor under transient excitation. The fixed end reflection signal was very strong, while the reflected signal from the embedded end was weak. This is mainly caused by attenuation of both the fixed reflection signal and the stress wave. The stress wave velocity characteristics in the soil anchor were between the values of anchorage medium materials and free anchors. The velocity is not only related to the characteristics of the bolt body and anchorage medium, but also to the adhesive strength between the bolt and anchorage medium.

Keywords: *dynamic waveform; nondestructive testing; reflection signal; soil anchor; stress wave velocity.*

1 Introduction

Bolt anchorage technology is widely used in several engineering fields such as coal mine roadways, railways, subway tunnels, civil air defense systems, water conservation installations and foundations. The anchor reinforcement technique has also been primitively applied to rock. Because soil anchors have several advantages, including low cost, simple processing [1], and convenient installation, they can increase the speed of construction and have the characteristics [2-3] of strong adaptation to soil and a small footprint, which are conducive to the construction process. Additionally, this technology has many applications in foundation pit engineering, anti-floating engineering and other fields [4-5].

However, due to the concealment of the soil anchor and the complexity of the working environment, there are several uncertainties regarding their design, construction and management. In use, prestress losses, slurry and geotextile

Received March 29th, 2015, 1st Revision June 22nd 2015, 2nd Revision July 15th, 2015, Accepted for publication October 13th, 2015.
 ISSN: 2337-5779, DOI: 10.5614/j.eng.technol.sci.2015.47.6.3

cause erosion, fractures and debonding, all of which seriously affect the normal working capabilities of the bolt. However, to date little attention has been devoted to their quality and static testing is rare [6]. This lack of research implies hidden trouble for engineering purposes, quality and safety. Presently, many scholars rely only on bolt drawing test studies [7-8], however it should be noted that dynamic measurement research has obtained certain achievements concerning rock bolts [9-11]. Soil can possess heterogeneity, high compressibility and high water content, and the soil anchor environment obviously differs from that of the rock anchor, so therefore it is necessary to use a dynamic measurement technique to study and discuss this problem [12-13]. As such, in this research we analyzed the change rule of soil anchor dynamic waveform measurements and we investigated the variable characteristics of the stress wave velocity on the key parameters to evaluate bolt anchoring. We present a relationship between the anchoring medium strength and the anchoring quality [14-15], which provides the basis for non-destructive soil anchor testing [16].

2 The Transmission of Elastic Stress Waves

When an elastic stress wave arrives, two types of wave impedance form at the interface of different media. This is produced through reflection disturbance and forms through the reflection of stress waves. Stress waves propagate in a bolt after the anchor end is subjected to a transient impact. If any wave impedance surface changes, the incident wave will reflect and transmit. In the wave-impedance interface, the original medium density of the upper part, the propagation velocity and the cross sectional area of a stress wave in the medium are ρ_1, A_1 and C_1, respectively. The original medium density of the lower part, the propagation velocity and the cross sectional area of a stress wave in the medium are ρ_2, A_2 and C_2, respectively. According to Newton's Third Law, under continuous conditions, the total force due to stress generated and the particle velocities are:

$$v_r + v_i = v_t \tag{1}$$

$$A_1(\sigma_r + \sigma_i) = A_2\sigma_t \tag{2}$$

where v_r, v_i and v_t, are the wave disturbance, incident wave disturbance and transmission wave disturbance caused by the particle velocities, respectively. σ_r , σ_i and σ_t , are the wave disturbance, incident wave disturbance and transmitted wave disturbance generated by the incident wave particle stress, respectively.

According to the conservation condition of a wave front, the total force can be written as:

$$\frac{\sigma_i}{\rho_1 C_1} - \frac{\sigma_r}{\rho_1 C_1} = \frac{\sigma_t}{\rho_2 C_2} \tag{3}$$

By combining Eqs. (2) and (3) we can obtain the particle stress produced by the disturbance of an incident wave disturbance and by the disturbance of a reflection wave and a transmission wave:

$$\sigma_r = \frac{\rho_2 C_2 A_2 - \rho_1 C_1 A_1}{\rho_2 C_2 A_2 + \rho_1 C_1 A_1}\sigma_i \tag{4}$$

$$\sigma_t = \frac{2\rho_2 C_2 A_2}{\rho_2 C_2 A_2 + \rho_1 C_1 A_1}\sigma_i \tag{5}$$

Introducing the wave impedance, *Z*, and the generalized wave impedance ratio, *n*, we obtain the available reflection coefficient, *F*, and the refraction coefficient, *T*:

$$F = \frac{1-n}{1+n} \tag{6}$$

$$T = \frac{2}{1+n} \tag{7}$$

$$n = \frac{Z_1}{Z_2} = \frac{\rho_1 C_1 A_1}{\rho_2 C_2 A_2} \tag{8}$$

$$Z = \rho C A \tag{9}$$

3 Model Design and Testing

3.1 Model Design and Production

A model anchor consisting of six embedded anchors was placed in different anchoring media and anchoring states. The model size was $600mm \times 600mm \times 2400mm$. The model cross section and arrangement are shown in Figure 1, where the anchor and section numbers correspond to: TM-1, TM-2, TM-3, TM-4, TM-5 and TM-6. The complete anchor TM-4 was the object of this research. Our experiments mainly analyzed the dynamic signal of soil layer anchor rods of different ages and the changing characteristics of the stress wave velocity. TM-4 was placed in a mortar to slurry ratio of 1:2, which acted as the anchoring medium, and purple soil played the role of the surrounding rock. The anchoring body was a rebar of 28 mm diameter, a free length (L1) of 0.1 m, and an anchorage length (L2) of 1.9 m. In order to compare the anchor stress wave velocity with the strength of the anchorage medium, a standard mortar test block of size $70.7mm \times 70.7mm \times 70.7mm$ was used.

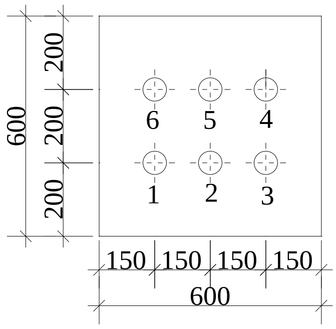

(a) Model section diagram.

(b) Indoor model diagram.

Figure 1 Soil anchor model.

3.2 Testing and Calculation of Stress Wave Velocity

3.2.1 Testing and Calculation of Stress Wave Velocity in the Anchor

Bolt testing was based on the stress wave reflection method. A vertical vibration that was anchored outside delivered the impact load, while an end sensor received the signal and a dynamic testing analyzer processed and analyzed the signal. The anchor structure of the signal is shown in Figure 2, the anchoring length being L2 and the bolt's free length L1. According to the dynamic signal measurement, by using the reflection time, *t*, of the bolt at the bottom and the fixed end reflection time, t_1, the propagation velocity of the stimulated stress wave in the bolt can be calculated as:

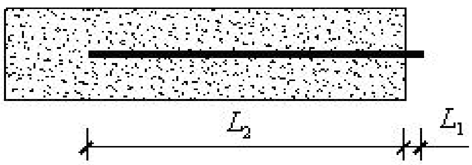

Figure 2 Structural scheme.

$$c = \frac{2L_2}{t - t_1} \tag{10}$$

3.2.2 Testing of Anchorage Medium Stress Wave Velocity

In each test stage, the compressive strength test was carried out on a group of three mortar samples. The average compressive strength of each of the three pieces was determined, which was used as a proxy for the compressive strength of each specimen. We measured the wave velocity of a mortar reference block using the ZBL-U520 nonmetal ultrasonic detector.

4 Results and Analysis

4.1 Acceleration Response Curve Characteristics of the Bolt

Different values of the generalized wave impedance ratio, n, reflection coefficient, F, refractive index, T, and the dynamic signal, have different characteristics when the elastic stress wave spreads from one medium to another: (1) if $n < 1$, then $T > 1$, $F > 0$, and the transmission disturbance surpasses the incident disturbance; (2) if $n > 1$, then $F < 0$, $T < 1$, and the transmission disturbance is weaker than the incident disturbance; and (3) when $n = 1$, $T = 1$, $F = 0$, the stress wave propagation does not spread along the bolt axial until it reaches the bottom of the anchor when the reflection occurs. Our analysis showed that A and B in Figure 3 represent the first wave signal and the bottom reflection, respectively.

When a wave travels in a bolt, not only do transmission and reflection occur, but there can also be constant attenuation. From the characteristics of stress wave propagation in a medium, it is known that when the wave impedance changes in a bolt, reflection and transmission will occur, and the transmission amplitude values are closely associated with the change of the wave impedance. The properties of the material within an anchor, or its cross sectional area, change greatly at the fixed end, so that a very strong reflection signal is expressed at the fixed end (in Figure 3) that has a great influence on the fixed end reflection signal, which makes the signal at the bottom quite weak. In addition, when a stress wave reaches the anchoring section, part of the energy can spread, scatter or be absorbed by the surrounding medium. This leads to a constant attenuation of the stress wave with an increase in propagation distance, which eventually undermines the bottom reflection signal, so that the reflection signal at the fixed end is weak, as shown in Figure 3. To summarize, the measurements showed that the signal characteristics of soil layer anchor TM-4 were that the fixed end reflection signal was very strong and the bottom of the reflected signal was weak.

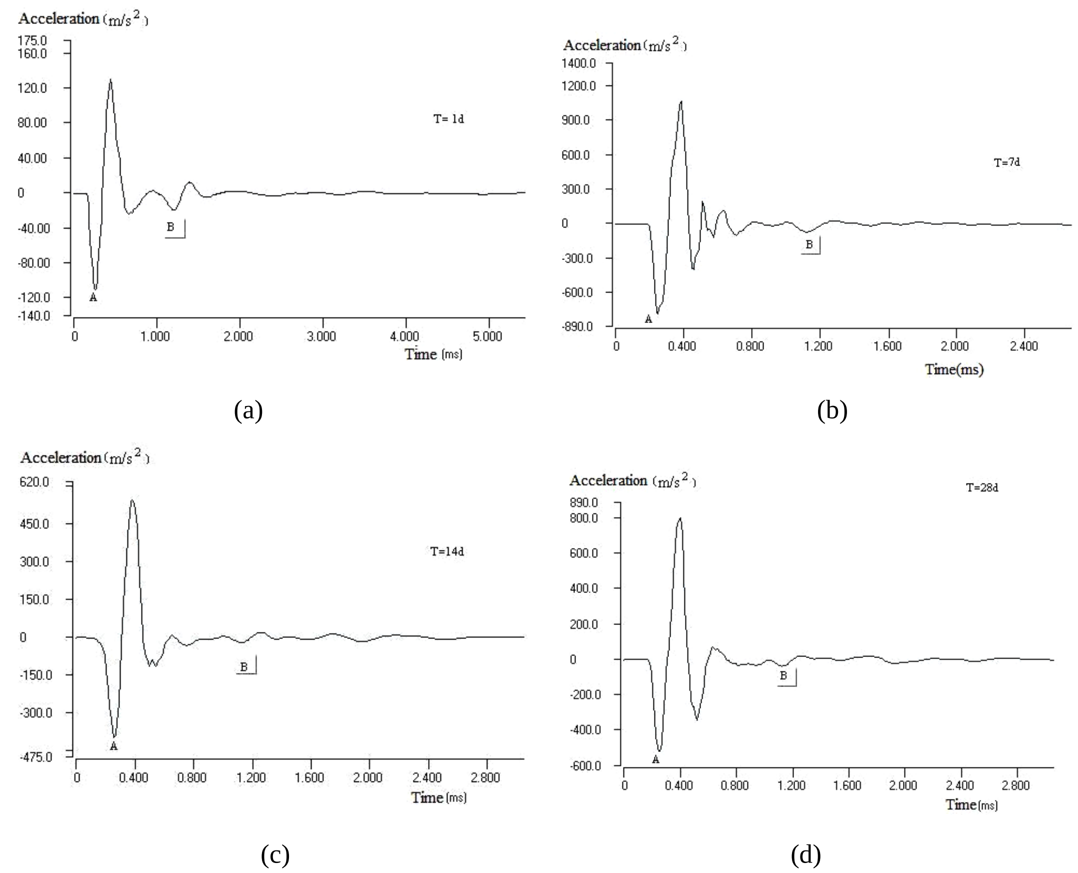

Figure 3 Acceleration responses in anchor TM-4 at various curing times.

4.2 Variable Characteristics of a Stress Wave

4.2.1 Stress Wave in Elastic Medium

If a medium is homogeneous, isotropic, continuous and perfectly elastic, and if we ignore the influence due to damping, stress wave propagation in a medium can be expressed in the following three-dimensional wave equation:

$$\rho\frac{\partial^2\varepsilon}{\partial t^2}-c^2\left(\frac{\partial^2\varepsilon}{\partial x^2}+\frac{\partial^2\varepsilon}{\partial y^2}+\frac{\partial^2\varepsilon}{\partial z^2}\right)=0 \tag{11}$$

where ε is the strain, t is the time variable, c is the stress wave velocity; the wave velocity is related to the elastic modulus, E, the medium density, ρ, and the Poisson ratio, μ.

For an elastic medium, if the axial size of the component is much smaller than the horizontal component, this can be regarded as a one-dimensional strain problem, where the wave velocity can be expressed as:

$$c = \sqrt{\frac{E(1-\mu)}{\rho(1+\mu)(1-2\mu)}} \tag{12}$$

If the axial size of the component is far greater than the horizontal component, this can also be regarded as a one-dimensional strain problem, and the wave velocity can be approximately expressed as:

$$C_0 = \sqrt{\frac{E}{\rho}} \tag{13}$$

When the elastic stress wave propagates along the combination surface of two kinds of media, the wave velocity will be not the same as that in just one of the media. Instead, it should be between them because of the constraints of the two different media.

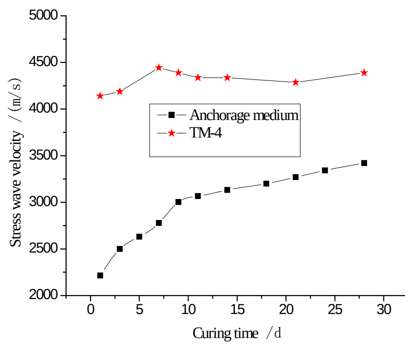

Figure 4 Relationship between stress wave velocity in anchor/anchorage medium and curing time.

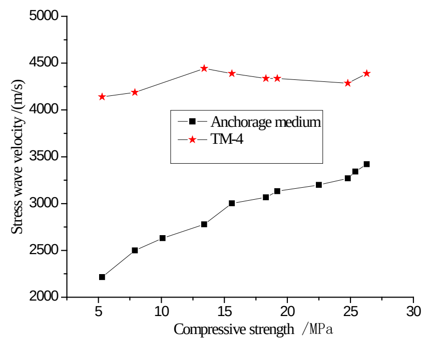

Figure 5 Relationship between stress wave velocity in anchor TM-4/anchorage medium and strength.

4.2.2 Variable Characteristics of Stress Wave in Anchorage Medium and Bolt

Figures 4 and 5 show that the anchorage stress wave propagation in the medium increased constantly. The wave velocity increased rapidly in the early stages, especially in the first seven days. At later times, the rate of increase was less high. The reason for this change is that the stress wave in an elastic medium has a close relationship with the elastic modulus of the medium, as seen in Equations (12) and (13). The elastic modulus of the mortar increases and especially in the early stages its strength and elastic modulus increase rapidly, while in the latter stages it only increases slowly with an increase of age, so that the early wave velocity increases rapidly and the later increases slowly.

Figures 4 and 5 also show that the bonding strength of the anchor rod body and the anchorage medium will increase, while the bolt stress wave and stress wave in an anchorage medium varies with age and strength. The wave velocity increased slightly in the first seven days, while the wave velocity obviously decreased. Eventually the wave velocity changed into a straight line from day 7 to day 14, while the wave velocity increased slightly later on, but the bolt stress wave velocity was always between the anchor medium wave velocity and the free anchor wave velocity. The main reason that the bolt stress wave velocity changed is because the mortar had not yet fully hardened after the completion of grouting, thus the bolt should be seen as two separate materials. Owing to the transient excitation loads on the bar, the wave velocity in the bolt is close to that of the wave velocity in steel, where the wave in steel spreads faster, so that the early wave velocity is large. As the mortar gradually hardens, the bonding strength of the mortar and the reinforcing steel bar increases, and the anchor medium, under transient excitation, and the steel bar vibrate simultaneously, with the increase in age. Meanwhile, the bolt stress wave velocity can be regarded as stress wave propagation in the two kinds of material (mortar and reinforcing steel bar composite materials rather than a single material) and the stress wave velocity is between that of both materials.

5 Conclusions

In this article, the following conclusions can be drawn based on our indoor nondestructive testing study of a soil layer anchor.

When it was under transient excitation, owing to the influence of fixed end stress wave reflection and attenuation, the variable characteristics of the soil layer anchor dynamic signal showed that the fixed end reflection signal was very strong and the bottom of the reflection signal was weak.

Due to different ages of the bolts, the variable characteristics of a stress wave in the soil anchor showed that the size of the wave velocity was between the stress wave velocity in the anchorage medium and in the free bolt. The size of the wave velocity is not only related to the bolt and anchorage medium, but also to the bond strength between them.

Because of the complexity and uncertainty of the soil layer anchor working environment, this article can be regarded as a preliminary study of the dynamic measuring signal and variable characteristics of the wave velocity. Additional research regarding other dynamic parameters, such as the damping ratio, dynamic stiffness and the variable characteristics of the fundamental frequency, require further development.

Acknowledgments

The authors would like to acknowledge the support of the National Natural Science Foundation of China (No. 51204098), the Scientific Research Fund of the Natural Science Foundation of Hunan Province, China (No. 11JJ6045).

References

[1] Kang, H.P., Wang, J.H. & Lin, J., *Case Studies of Rock Bolting in Coal Mine Roadways*, Chinese Journal of Rock Mechanics and Engineering, **29**(4), pp. 649-664, 2010.

[2] Wang, B.Q. & Meng, Y.M., *Analysis by Model Test on Anchors in Clay*, Journal of Earth Sciences and Environment, **31**(2), pp. 195-199, 2009.

[3] Duan, J., Yan, Z.X. & Guo, R.J., *Analysis of Anchorage Characteristics and Parameter Influence of Soil Imperfect Anchor*, Journal of Central South University (Science and Technology), **43**(8), pp. 3209-3215, 2012.

[4] Hao, J.B., Meng, Y.M. & Wang, B.Q., *Working Property of Soil Anchors under Loads on Ground Surface*, Chinese Journal of Geotechnical Engineering, **31**(2), pp. 247-249, 2009.

[5] Jeng, F.S. & Huang, T.H., *The Holding Mechanism of Under-Reamed Rock Bolts in Soft Rock*, International Journal of Rock Mechanics & Mining Sciences, **36**, pp. 761-775, 1999.

[6] Kilic, A., Yasar, E. & Atis, C.D., *Effect of Bar Shape on the Pull-Out Capacity of Fully Grouted Rockbolts*, Tunnelling and Underground Space Technology, **18**, pp. 1-6, 2003.

[7] Kilic, A., Yasar, E. & Atis, C.D., *Effect of Bar Shape on the Pull-Out Capacity of Fully Grouted Rockbolts*, Tunnelling and Underground Space Technology, **17**, pp. 335-362, 2000.

[8] Wang, B.Q. & Meng, Y.M., *Analysis by Model Test on Anchors in Clay, Journal of Earth Sciences and Environment*, **21**(1), pp. 126-129, 2002.

[9] Zou, D.H. Cui, Y. & Madenga, V., *Effects of Frequency and Grouted Length on the Behavior of Guided Ultrasonic Waves in Rock Bolts*, International Journal of Rock Mechanics & Mining Sciences, **40**, pp. 813-819, 2007.

[10] Zhang, C.S., Zou, D.H. & Madenga, V., *Numerical Simulation of Wave Propagation in Grouted Rock Bolts and the Effects of Mesh Density and Wave Frequency*, International Journal of Rock Mechanics & Mining Sciences, **43**(4), pp. 634-63, 2006.

[11] Madenga, V., Zou, D.H. & Zhang, C.S., *Effects of Curing Time and Frequency on Ultrasonic Wave Velocity in Grouted Rock Bolts*, Journal of Applied Geophysics, **59**, pp.79-87, 2006.

[12] Chen, J.G. & Zhang, Y.X., *Analysis on Characteristics of Dynamic Signal for Bolt Anchorage System*, Chinese Journal of Geotechnical Engineering, **30**(7), pp. 1051-1057, 2008.

[13] Sun, B., Zeng, S. & Ding, D.X., *Research on Transmit Rules of Stress Wave with Low Strain in Dynamic Test Pile and Anchorage Bolt*, Rock and Soil Mechanics, **32**(4), pp.1143-1148, 2011.

[14] Beard, M.D. & Lowe, M.J.S., *Non-Destructive Testing of Using Guided Ultrasonic Waves*, International Journal of Rock Mechanics and Mining Sciences, **40**, pp. 527-536, 2003.

[15] Cui, Y. & Zou, D.H., *Numerical Simulation of Attenuation and Group Velocity of Guided Ultrasonic Wave in Grouted Rock Bolts*, Journal of Applied Geophysics, **59**, pp. 3337-344, 2006.

[16] Li, Y., Zhang, C.S. & Wang, C., *Study on Several Key Issues in Nondestructive Detection of Bolt Bonding Integrality*, Chinese Journal of Rock Mechanics Engineering, **27**(1), pp. 108-116, 2008.